Published in final edited form as:
J Cardiovasc Transl Res. 2014 November ; 7(8): 756–767. doi:10.1007/s12265-014-9593-1.

A Needleless Liquid Jet Injection Delivery Method for Cardiac Gene Therapy: A Comparative Evaluation Versus Standard Routes of Delivery Reveals Enhanced Therapeutic Retention and Cardiac Specific Gene Expression

AS Fargnoli[1,2], **MG Katz**[1], **RD Williams**[1], **KB Margulies**[3], and **CR Bridges**[1]

[1]Sanger Heart & Vascular Institute, Thoracic and Cardiac Surgery, Carolinas Healthcare System: Charlotte NC

[2]School of Engineering and Applied Science, Bioengineering, University of Pennsylvania: Philadelphia PA

[3]Perlman School of Medicine, Internal Medicine, University of Pennsylvania: Philadelphia PA

Abstract

Background—This study evaluates needleless liquid jet method and compares it with three common experimental methods: (1) Intramuscular injection (IM) (2) Left ventricular intracavitary infusion (LVIC) (3) LV intracavitary infusion with aortic and pulmonary occlusion (LVIC-OCCL).

Methods and Results—Two protocols were executed. First, [n=24 rats], retention of dye was evaluated 10 minutes after delivery in an acute model. The acute study revealed the following: significantly higher dye retention (expressed as % myocardial cross section area) in the left ventricle in both the Liquid Jet [52±4] % and LVIC-OCCL [58±3] % groups $p<0.05$ compared with IM [31±8] % and LVIC [35±4] %. In the second, [n=16 rats], each animal received AAV.EGFP at a single dose with terminal 6 week endpoint. In the second phase with AAV.EGFP at 6 weeks post-delivery, a similar trend was found with Liquid Jet [54±5] % and LVIC-OCCL [60±8] % featuring more LV expression as compared with IM [30±9] % and LVIC [23±9] %. The IM and LVIC-OCCL cross sections revealed myocardial fibrosis.

Conclusions—With more detailed development in future model studies, needleless liquid jet delivery offers a promising strategy to improve direct myocardial delivery.

Keywords

Gene Therapy; Myocardial injection; Drug Delivery; Devices

Corresponding Author: Dr. Charles R. Bridges, Carolinas Healthcare System, Thoracic and Cardiac Surgery, Cannon Research Center, 1542 Garden Terrace, Charlotte NC 28203. Charles.Bridges@carolinashealthcare.org 215.829.8719 (voice).

DISCLOSURE STATEMENT
No competing financial interests exist.

INTRODUCTION

Heart failure (HF) remains a significant burden to the global healthcare system with annual costs exceeding $32 billion [1]. Besides the limited number of donor organs available for transplantation, current medical and device therapies have not significantly reduced disease burden. Through careful scientific investigation and clinical development, gene therapy has emerged as a promising strategy to directly treat myocyte dysfunction at the molecular level. A number of genes have been identified to impact these critical disease pathways - which if expressed robustly in the myocardium - enhance contractility, promote survival, and in some cases completely reverse chronic HF [2–4]. Adding to this momentum, novel microRNA and angiogenesis targets promoting genetically induced regeneration are accelerating through various developmental stages [5,6]. Therefore, the recent basic scientific progress has bolstered an already thriving pipeline of viral mediated gene therapeutics and it is expected that new clinical trials will be forthcoming.

A pivotal milestone for the cardiovascular gene therapy field was the successful launch of the Calcium Up-regulation by Percutaneous Administration of Gene Therapy in Cardiac Disease (CUPID) trial featuring adeno-associated viral vector (AAV) encoding the contractility enhancing sarcoplasmic endoreticulum ATPase (SERCA2a) gene [7]. This key trial has provided reason for cautious optimism as favorable results were achieved in the high dose group versus placebo [7,8]. Despite these encouraging results in the high dose group, achieving efficacy with lower doses remains a concern given that no improvement was found in patients receiving less than the maximum 1×10^{13} DNAase resistant viral particles (vp) [8]. Delivery efficiency is the main concern, whereby higher doses are needed to achieve sufficient expression levels for greater outcome measures, which inherently increases the risk for adverse events. Therefore, more efficient delivery systems would most likely improve clinical outcomes.

The administration route currently practiced in clinical trials is antegrade intracoronary infusion. This choice is attributed to its safe and effective implementation in clinical practice, which is feasible to implement in moderate to high risk heart disease patients [9]. From a therapeutic AAV biotransport perspective however, standard infusion approaches are critically limited by these factors: (1) Prohibitive physical barriers (e.g. pre-capillary sphincters and endothelial barriers) preventing viral vector diffusion into the interstitial compartment [10] (2) Plaques and inflammatory elements in primary vessels, which are common in patients with advanced coronary disease (3) Neutralizing antibodies and blood components which limit viral particle bioavailability prior to interstitial compartment entry [11] (4) Inadvertent systemic exposure and uptake in collateral organs and finally (5) The exclusion of many patients seropositive for AAV. Sophisticated modifications to percutaneous catheter infusion (e.g. single or concomitant retrograde/antegrade balloon occlusion systems [12] and even surgical closed loop recirculation systems [13]) have been advanced recently to increase efficiency at the cost of complexity. Some of these systems may be implemented in future trials, however most would either exclude high risk patients or impose additional safety concerns.

An alternative to infusion methods in an effort to improve efficiency and cardiac specificity is direct myocardial delivery. Direct injection methods circumvent the blood and anatomical barriers by directly administering the product into the myocardium. This approach additionally offers the advantage of precise site selection. For this reason direct intramuscular (IM) injections were attempted with adenovirus in the very first series of angiogenesis trials [14], but yielded poor results. Cited problems with this route are limited distribution per needle injection site and inflammatory responses with repetitive injections in a local cardiac region [15,16]. There has been little work to date to improve direct myocardial delivery applications, despite the need for greater cardiac specificity.

In this study we present a novel approach to add to the repertoire of direct cardiac gene delivery approaches using a needleless liquid jet methodology. Similar ballistic delivery methods were utilized in very early DNA transfection studies via gene gun [17,18], but to date none have attempted delivery of AAV therapeutics as a potential clinical strategy. The liquid jet application is essentially a device concept that accelerates and disperses the therapeutic at a targeted myocardial site. The core hypothesis offered is that this approach can be optimized for a cardiac application and could result in: increased therapeutic retention in the initial delivery phase (i.e. microjets with smaller volume payloads will increase retention versus large bolus profile of IM), achieve significantly more total myocardial expression per dose, and in addition yield a more homogenous distribution profile similar to infusion methods. For direct injection methodologies this would be a significant advancement, since there is an unmet need to increase efficiency per delivery site while simultaneously decreasing adverse events such as systemic exposure and local injury.

More comprehensive myocardial gene delivery studies are required to optimize current and future applications. This proof of principle study optimizes the needleless liquid jet strategy for cardiac applications and evaluates the method in a series of rodent experiments. In each set of experiments, the liquid jet method is compared with three existing methods: Intramuscular injection (IM), Single pass LV intracavitary infusion (LVIC) infusion, and LV intracavitary infusion with aortic and pulmonary artery occlusion (LVIC-OCCL) to mimic the advanced methods that use occlusion techniques to increase therapeutic transfer via enhanced local pressure and residence time. In the first series of experiments we evaluate each methodology’s immediate myocardial retention profile in an acute model. In the second series, we utilize a highly cardiotrophic AAV.EGFP marker gene construct to simulate a more realistic long term gene expression scenario at 6 weeks. We evaluate, compare and discuss the risk/benefit ratio of each method in terms of actual gene expression achieved as a percentage of myocardial coverage against early evidence of myocardial damage in addition to collateral organ uptake.

MATERIALS AND METHODS

Animal Care and Handling

40 rats were procured from Charles River Laboratories and handled in accordance with IACUC guidelines at the Cannon Research Center at Carolinas HealthCare System to support the two delivery studies. Normal Sprague Dawley rats (males, weight 300 g) were

obtained for all experiments and screened with a health assessment. Animals were assigned to various delivery groups in equal number, but not in a randomized manner.

Needleless Liquid Jet Injection Device Optimization & Specifications

A DermoJet™ liquid jet device (Robbins Instruments, Chatham NJ) was acquired and modified for cardiac delivery applications. The spring actuator length was reduced by 80% to 1.9 cm, which resulted in a significant driving power reduction. A super speed camera (Zeiss International, Thornwood NY) at the University of Pennsylvania Complex Fluids Laboratory was used in a custom analysis suite to quantify jet fluid exit velocity and to compute estimated driving pressure. The nozzle jet velocity was measured at 110 m/s based on a 30,000 images per second capture rate. The driving pressure ranged from 150 – 250 kilopascals (kPa). Prior to the modification, the factory setting results were 330 m/s velocity at greater than 550 kPa.

The next key parameter to optimize for a surgical application was the injector head distance normal to the target cardiac plane. To execute, the pen configuration injector was mounted to a stainless steel arm apparatus secured to a solid base. For alignment with the cardiac targeted surface plane, an optical system consisting of a field laser and digital level were utilized in conjunction to ensure accuracy between injections.

The safe liquid jet delivery distance range was determined by performing a limited number of acute studies with methylene blue dye injection. Safety criteria were defined as tolerance of 6 consecutive projected needleless injections without visible bleeding and EGC changes. Confirmation of hits was validated via marks by surface retention of dye. The optimal distance range was determined between 8–10 inches (i.e. nozzle tip to heart surface). This range was found effective where sufficient dye was retained transmurally, but no incidence of major cardiac damage was observed.

Rhodamin B Dye Preparation for Acute Studies

A total of 24 rats, 6 per delivery group were assigned for this first study phase. Rhodamin B Dye (Sigma Aldrich, St. Louis MO) was prepared in (50 μg/mL) working aliquot concentration. Rhodamin B dye was selected based on easy formulation and high performance in muscle tissue types for the acute retention purpose.

AAV.EGFP Viral Vector Production for Survival Studies

All Recombinant AAV.EGFP was sourced from the University of Pennsylvania Vector Core (Philadelphia, PA). Briefly, vector production, harvest, purification and testing were done from cell lysates by the Penn Vector Core. The recombinant vector used in this study contains an AAV serotype-9 viral capsid and a single strand: ~4.5-kb DNA containing the EGFP marker gene driven by a cytomegalovirus immediate-early promoter/enhancer, a hybrid intron, and a bovine growth hormone polyadenylation signal. Manufacturing process details can be found (http://www.med.upenn.edu/gtp/vectorcore/). Following production, viral preps were pooled from individual lots and aliquoted in sterile vials each containing a dose of 2×10^{11} vp in 500μL volume.

Acute Model Protocol: Retention of Rhodamin Dye

The endpoint selected for retention in the cardiac cross sections was % myocardial area positive for Rhodamin B dye level 10 minutes following cardiac delivery. Since global, homogenous distribution is the ideal outcome for contractility genes, this measure essentially determines what areas of myocardium are accessed per route.

All rats were anesthetized with ketamine IM, intubated and placed on a Harvard Apparatus ventilator and maintained with isoflourane 1–3%. A left thoracotomy was performed and the pericardium excised to expose the beating heart. Each animal was then assigned to 1 of 4 acute delivery groups (n=6 each) [IM Injection, Needleless Liquid Jet, LVIC-OCCL, LVIC)] to receive a single 500μL fixed dose Rhodamin B Dye. A 10 minute waiting period commenced after delivery. The heart was then harvested and sectioned immediately following.

Delivery Method Execution

A conceptualized illustration of all 4 cardiac delivery approaches of IM Injection (Figure 1A), Needleless Liquid Jet injection (Figure 1B), Left ventricular single pass infusion (LVIC) (Figure 1C) and Left ventricular infusion with concomitant occlusion of the aorta and pulmonary vessels (LVIC-OCCL) (Figure 1D).

The technical delivery details for execution in the rodent model were as follows:

IM Injection—A 1 mL 30 gauge syringe was loaded with the 500μL of volume. Injection sites on the left ventricular apex, anterior wall, and lateral wall were marked with a surgical pen. Two injections were performed in the mid-ventricular plane for each of the anterior and lateral walls, with a single injection in the apex for 5 total injections. Injections were spaced about 5 mm.

Needleless Liquid Jet Injection—500μL delivery volume was loaded into the chamber with a residual capacity of at least 200μL additional to ensure the 5th shot maintained the same kinetics as per DermoJet™ manufacturer instructions. A digital level and laser was used to ensure adequate degree and plane alignment with the middle left ventricular plane. Five separate shots, each containing 100μL, were fired perpendicular to the LV surface. Hits were confirmed by detection of pinhole piercing on the epicardial surface with surrounding coloration changes.

LVIC-OCCL Infusion—Silk suture was placed in two locations, the proximal aortic arch and the left pulmonary artery. Following, a 16 gauge needle introducer was used to catheterize the left ventricle from the apex. A catheter was secured in place with a syringe containing the 500μL of therapeutic. Just prior to infusion, concomitant occlusion of both snares with slow infusion was conducted over a 10 second period. The occluding sutures were then released after the 10 second period.

LVIC Infusion—A 16 gauge needle introducer was used to catheterize the left ventricle from the apex. A catheter was secured in place with a syringe containing the 500μL of

therapeutic. Slow infusion in the left ventricle over 10 seconds was performed without interruption.

Survival Model Protocol: Expression Profile Following Delivery of AAV.EGFP

A total of 16 rats, 4 per delivery group were assigned for this second study phase. All rats were anesthetized with ketamine IM, intubated and placed on a Harvard Apparatus ventilator and maintained with isoflourane 1–3%. A left thoracotomy was performed and the pericardium excised to expose the beating heart under aseptic conditions. Each animal was then assigned to 1 of 4 delivery groups (n=4 each) following the same delivery protocol for [IM Injection, Needleless Liquid Jet, LVIC-OCCL, LVIC)] groups. The therapeutic was a single 500μL fixed dose 2×10^{11} (vp) of single stranded adeno-associated virus encoding green fluorescent protein (AAV9.EGFP). Following delivery, the incision was closed and each animal was recovered and monitored to 6 weeks. At the 6 week peak expression endpoint, the harvest commenced.

Tissue Harvest and Cross Section Preparation

For each animal 3 distinct left ventricular cross sections were acquired: Apex, Middle, and Basal planes spaced 3mm apart. A single liver section was also acquired. All cross sections were snap frozen in OCT. Ten micron sections were cut on a cryostat and mounted on glass slides for further analysis.

Immunohistochemistry Staining for EGFP Detection

Tissue from rats receiving the AAV.EGFP was stained with a rabbit polyclonal Anti-GFP antibody (Abcam ab-290). Bound antibody was detected with an ImmPRESS anti-Rabbit kit (Vector Labs MP-7401) and visualized with ImmPACT VIP chromagen (SK-4605). Cells were counter stained with methyl green.

Masson's Trichrome Staining for Myocardial Fibrosis at 6 Weeks Post Delivery

Formalin fixed paraffin embedded tissues were sectioned at 4 microns on a Leica RM2125 microtome, picked up on Plus slides and air dried overnight. Slides were then baked in a 60 degree oven for 20 minutes to remove excess paraffin before being deparaffinized and with xylene and rehydrated with several changes of graded alcohol to distilled water. H&E sections were stained with Mayer's hematoxylin for 20 minutes, rinsed with running tap water and stained with Eosin Y for 5 seconds followed by several rinses in 95% alcohol. Masson's Trichrome slides were stained with Weigert's Iron Hematoxylin for 10 minutes followed by a rinse in tap water. The rest of the staining was done with a Masson's Trichrome kit purchased from Polyscientific (Bay Shore, NY cat# k037). The slides were then dehydrated with several changes of graded alcohol and cleared with xylene before being coverslipped with Permount.

Cross Section Image Capture

Images of each animal's respective middle and basal left ventricular cross sections were obtained using an Olympus BX40 microscope with a DP72 camera and CellSens software with fixed acquisition settings at 4 × magnification. Multiple images at 4x were stitched to

reconstruct a complete 2D cross section for heart and liver per animal per region. Slides of unstained cross section tissue from rats receiving Rhodamin B were imaged under 540nm fluorescence. Basic light microscopy was used with the same approach as described above for the EGFP sections, however without fluorescence as positive GFP detection was indicated by brown-purple stain hues.

Imaging Analysis Protocol

Following acquisition, the middle LV, basal LV, and liver cross section images were standardized with a custom Java programmed macro in ImageJ software to apply uniform brightness, contrast and sharpness settings. Quality control checks of pixel density, resolution, and image size were done prior to analysis. All images were saved into Grayscale 16 bit format and blinded for analysis.

Cardiac Cross Section Analysis—Each middle LV, basal LV and liver cross section was loaded into ImageJ. For the Rhodamin B fluorescent images only, each cross section was first subtracted from saline control templates to minimize the background effect. The Iterative self-organizing data analysis technique (ISODATA) algorithm was utilized to determine the threshold for positive therapeutic (Rhodamin B or EGFP positive pixels). Briefly, the algorithm mathematically derives the statistically validated threshold based on the normal distribution sampling of all pixel intensity values and arrives at an optimal detection value [19].

Following ISODATA identification, the 16 bit Grayscale images were converted into binary, whereby all pixel values above the computed threshold were scored positive. Two myocardial contours were drawn, one for the outer epicardial border and another for the inner endocardial surface. The pixel values contained within the endocardial contour were voided prior to computation. The percentage positive therapeutic area was defined as follows for the cross sectional myocardium:

$$\%\,(+)\,\text{Positive Score}=\frac{\#\,\text{Positive Therapeutic Pixels}}{\#\,\text{Pixels in Outer Area}-\#\,\text{Pixels in Inner Area}}\times 100$$

Liver Cross Section Analysis—The cross sectional images were handled the same as described above, however scoring was focused on therapeutic intensities in the liver to gauge systemic uptake. First, as in above the percentage positive liver area was determined. Second, the grayscale Integrated density was determined by multiplying the gray value (1–255) for each pixel:

$$\sum_{1}^{\text{Total (+) Pixels}} \text{Gray Value}\times\text{Pixel Unit}$$

The final exposure score was computed as the mean gray value of all positive pixels determined from the algorithm (Integrated Density/Total Positive Pixels) X % affected area.

Therapeutic Transfer Score Reporting

Each middle LV, basal LV and liver cross section was scored individually. An overall cardiac transfer score was compiled by grouping middle and basal LV sections reported by delivery group. Likewise, systemic exposure score was reported per delivery group with the liver cross sections.

Needleless Liquid Jet Evaluation in Explanted Ovine Myocardium

To obtain a basic translational perspective on the optimized device, a basic methylene blue injection experiment was executed with post-harvest ovine left ventricle. 15 liquid jet injections each containing 100μL were fired from the device setup at a 4 inch distance to account for the greater thickness. Qualitative epicardial and endocardial wall penetration as well as coverage were observed.

Data Analysis and Statistics

All data are reported as mean ± standard error of the mean (SEM), per delivery group in each respective study. The Bartlett's test was used to verify equal variances within the delivery groups. Then, single way ANOVA was used to determine difference across all 4 groups with a post hoc Tukey's test to determine comparative difference between the groups at the 0.05 confidence level in the overall cardiac (i.e. either Rhodamin or EGFP) and liver systemic exposure scores. T-testing was used to determine difference between compiled direct delivery and infusion approaches and also differences between middle and basal LV sections in the delivery groups for the AAV.EGFP subjects.

RESULTS

Survival and Delivery Performance

All surgical procedures were successful both in terms of delivery objectives and reaching their designated euthanasia timepoints. There were no major abnormalities or ECG changes found intra or post operatively.

Rhodamin B Dye Acute Model Analysis

(Figure 2) illustrates the typical distribution profile per method from the Rhodamin B retention analysis. The images demonstrate both the degree of myocardial coverage and regional cross section peak intensities (e.g. mild red to hot yellow) as a function of delivery route. These results were consistent between subjects per group; supporting the claim that delivery route had a major influence on retention profile.

IM injection resulted in highly focal, heterogeneous cardiac delivery with a moderate degree of systemic exposure. By comparison, the liquid jet group demonstrated a more disperse, yet homogeneous pattern with higher intensities along the epicardial surface, but none has high as in the IM sections.

Conversely, the infusion groups demonstrated that increased retention is driven by induced pressure and residence time as there was a dramatic difference between the LVIC-OCCL and LVIC groups.

Single way ANOVA following a passed Bartlett's test for equal variances yielded a ($p=0.000115$). Quantitatively, the Liquid Jet [52±4] % (+) myocardial area group performed in a similar range with the LVIC-OCCL group [58±3] % (+). Both the Liquid Jet and LVIC-OCCL methods resulted higher distribution levels compared with the IM [31±9] % (+) and LVIC [35±4] % (+), $p<0.05$ confidence with Tukey's test (Figure 3A). All groups presented with varying degrees of systemic liver exposure, (Figure 3B) IM [37±7] arbitrary Rhodamin Units (AU), Liquid Jet [26±5] (AU), LVIC-OCCL [45±7] AU and LVIC [46±7] AU. The Liquid Jet group was the most cardiac specific.

When comparing direct (i.e. combined IM/Liquid Jet) versus infusion (i.e. combined LVIC/LVIC-OCCL), higher systemic liver exposure (Figure 3C) [46±5] AU as compared with direct injection methods [31±4] AU was found $p=0.014$.

AAV Mediated Cardiac EGFP Expression Analysis at 6 Weeks Post Delivery

Despite the profound size (Rhodamin dye 20–50Da; AAV 4×10^6 Da), diffusive properties and functional differences between dye and AAV, it was found that the overall distribution patterns for each delivery group generally matched those results found in the acute study. Overall cardiac AAV mediated GFP delivery in the heart was more effective with the Liquid Jet [54±5] % (+) and LVIC-OCCL [60±8] % (+) methods, both $p<0.05$ with Tukey's test as compared with the LVIC [23±9] % (+). In addition, the LVIC-OCCL method was found significantly better than the IM group IM [30±9] % (+).

A key number of findings were determined, specifically with respect to the EGFP distribution throughout the LV anatomy, indicative of methodology characteristics. (Figure 4) depicts representative whole left ventricular cross sections per group (i.e. higher basal and lower middle LV plane regions), whereby GFP detection is indicated with (brown/purple) stain while white/blue regions are devoid of any detectable expression. The results are summarized by group as follows:

IM Injection—The GFP distribution was localized around the primary injection sites, but in comparison to dye results the size and bioactivity of AAV permitted greater myocardial coverage in the middle region. The middle left ventricular region score was higher [46±2] % (+) than the basal region [13±12] % (+) $p=0.068$. This difference was most likely attributable to the consistent application of AAV into the middle left ventricular zone. Based on this difference, it is likely that not much product diffuses into regional distances beyond the site of injection.

Liquid Jet Injection—The needleless jet offered a robust, yet homogenous pattern of GFP expression with nearly equal levels in the basal and middle left ventricular sections indicating the jet profile's dispersive effects per shot. The scores were [54±8] % (+) in the middle and basal [56±9] % (+) regions, $p=0.39$. The intensity was generally greatest in the epicardial regions of site impact, although significant expression was found in the remote posterior wall regions indicating complete myocardial penetration.

LVIC-OCCL Infusion—This route offered the highest degree of expression in terms of both intensity and distribution of cross sectional GFP coverage. The score in the middle left

ventricular was the highest at [71±6] % (+). The basal region also scored high [50±14] % (+) and presented with a homogenous pattern, but no significant difference p=0.12. These model results recapitulate the importance of driving local pressure and residence time to maximize delivery through the coronary anatomy.

LVIC—The difference between expression levels between the anatomical regions was the most dramatic here, with the middle region scoring [41±6] % (+) while the basal region [5±3] % (+), p=0.016. These results suggest that very little retention in remote areas is achieved without increased pressure and residence time as compared with the LVIC-OCCL group.

AAV Mediated Collateral Liver EGFP Exposure Analysis at 6 Weeks Post Delivery

Single way ANOVA determined a significance in liver exposure scores, p=0.002. The Liquid Jet group [27±3] AU was the most cardiac specific resulting in a lower liver score versus the other 3 groups IM [71±10] AU, LVIC-OCCL [77±3] and LVIC [83±2] respectively, $p<0.05$ with Tukey's test.

Myocardial Injury from AAV.EGFP per Delivery Method

The IM Injection delivery group presented with significant detectable scarring in the anterior to posterior wall regions in 2/4 subjects. A representative image is shown in (Figure 5A). A lesser degree of damage but higher frequency 3/4 subjects was found in the LVIC-OCCL group (Figure 5B). In contrast to these results, the Liquid Jet and LVIC groups did not reveal any damage in the heart, (Figure 5C) and (Figure 5D) respectively. This data suggests that IM mediated AAV delivery imposes local injury risks from either the original event, the expression profile or in combination. The LVIC-OCCL injury was most likely caused by transient ischemic event induced from the 10 second occlusion interval.

Ex Vivo Ovine Myocardial Liquid Jet Injections

The selected epicardial injection distance for the proposed clinical equivalent was determined at 4 inches. This strike distance was found optimal since maximum myocardial coverage and retention transmurally, but not through the endocardium surface (i.e. complete LV wall retention). Figure 6 depicts primary impact sites shown on the epicardial surface (Figure 6A) and transmural retention shown from the reverse endocardial surface (Figure 6B). As expected the greater scale size factor imposes concerns for direct delivery.

DISCUSSION

Achieving sufficient myocardial expression through a selected vector, dose and delivery route treatment plan is balanced by the clinical implementation risks [20,21]. As demonstrated in this study, the choice of administration route can significantly impact the biodistribution and myocardial injury risks realized for cardiac gene therapy. The observations and discussion items presented here are inline with the clinical goal to obtain global, homogeneous delivery while minimizing systemic toxicity, which is an unresolved problem in clinical trials. The ideal cardiac gene delivery method would safely facilitate sufficient transduction levels, effectively promoting long term global rescue. The resultant

expression profile would also have to be sustainable and not induce host responses over a lifetime, since administration is performed in a single treatment. Fundamentally the results in this study demonstrate that route efficiency is paramount in achieving maximum myocardial expression. However just as important, the resultant expression level should be considered along with the collateral organ exposure and myocardial injury risks that each imposes. The initial delivery phase is largely influenced by physical transport principles (i.e. muscle properties, local trafficking vessel pressure, residence time, trafficking properties, mechanical resistance) that are independent of AAV characteristics and must be considered first. In conjunction with the anatomical constraints, the viral vector's molecular properties and transgene immunogenicity must also be considered when evaluating the risk/benefit ratio of the cardiac gene therapy strategy.

This development study demonstrates that a number of technical measures can be employed to increase gene distribution in the myocardium, as well as reduce systemic exposure in critical collateral organs such as the liver. As demonstrated in the LVIC-OCCL group for example, increased residence time and local pressure gradients significantly increase performance, but at the cost of a higher safety risk. The novel liquid jet approach offers a means to effectively distribute the AAV therapeutic while minimizing undesirable systemic uptake and myocardial injury risks, provided settings are optimized for the particular application. Two unresolved problems with IM injection wherein the needleless liquid jet approach may be beneficial are: to improve initial therapeutic retention and diminish the risk of subsequent host responses associated with local injury. With regard to the first problem, other studies have confirmed that a significant portion of the IM injection volume is either lost into the systemic circulation or back through the injection site itself [22–24]. This finding likely explains the variable results achieved between patients, since the beating heart represents a challenging dynamic target featuring accentuated changes in the structural wall thickness during delivery [25]. Altering the volume load per injection site may or may not improve outcomes since delivering a lower amount would logically demand additional injection sites for the same level of coverage.

The second challenging problem to resolve for cardiac gene delivery methods is the risk for chronic injury occurring at the time of initial delivery or resulting from the subsequent AAV-mediated expression biodistribution profile. In particular direct methods impose anatomical safety risks and concerns related to the resultant heterogeneous expression patterns. These taken together have been shown to cause inflammatory and adaptive immune reactions to gene therapy products [26]. Large animal studies utilizing IM injection with viral vector mediated expression have reported high incidence of myocarditis and T cell mediated immune responses [26]. In addition to the inflammation generated from multiple needle sticks, comprehensive studies have raised key concerns regarding the highly localized gene expression profile in muscle [26,27]. It has been shown that inflammation resulting from injury at the time of delivery and highly focal expression profile are interrelated in triggering subsequent immune responses long after the initial delivery period [28]. Both innate and adaptive immune responses following the initial delivery event are major concerns, especially since advanced heart failure patients present with severe degrees of chronic inflammation and fibrosis [29].

This study revealed that the IM injection and LVIC-OCCL methods impose moderate myocardial damage as compared with the liquid jet and intracoronary method without occlusion. Our fibrosis results indicate that 5 repeat injections with a 30 gauge needle are sufficient to induce long term irreversible LV damage. Although beyond the scope of this study, this damage may have been caused by the initial delivery event or focal GFP expression itself, or a combination of both risk factors. Expanding upon this point, other reports have confirmed that the pharmacodynamic effects with IM injections saturate to a biological limit [30,31], whereby expression levels beyond the therapeutic threshold provide no clinical benefit and actually increase immunogenicity risks with viral vector mediated products. Thus, with more detailed investigation the liquid jet methodology might become an attractive clinical application to achieve greater efficacy while at the same time minimizing the host response risks associated with systemic exposure and focal expression profiles.

Contrarily, infusion methods do not report issues with induced inflammatory responses; however do cite problems with transport efficiency from the primary infusion vessel and overall cardiac retention. These problems are attributed to atherosclerotic vessels and brief residence time, thus resulting in high systemic exposure levels. Despite healthy vessels in the normal rodent model, high levels of liver exposure were presented in both infusion groups, thus confirming this translational problem of restricting AAV to the myocardium. In response to this problem, increased interest in modified intracoronary catheter infusion approaches featuring pressure regulated balloon occlusion systems that attempt to increase performance have been implemented in large animal models [32,33]. These approaches have reported an increase in performance but it is controversial whether or not they can be implemented safely in high risk patients. This study confirms the risk of increasing driving pressure to increase performance while remaining within safe limits. This was evident when comparing the LVIC and LVIC with occlusion groups. In this example, ischemia resulting from the occlusions likely resulted in mild myocardial injury despite the greatest possible demonstrated GFP expression level.

Given the efficiency concerns with existing infusion methods, there could be a gradual shift toward more direct delivery applications such as liquid jet injection provided they are feasible clinically. The fundamental concept as stated previously is that direct applications essentially bypass restrictive vessel barriers which contain humoral components such as antibodies that limit vector bioavailability. There is a demand for these systems since greater than 50–65% of the general population has pre-existing immunity to one or more AAV serotypes preventing clinical trial enrollment [34]. The liquid jet application circumvents this problem by restricting gene therapies directly in the myocardial compartment, which is largely myocyte mass behind restrictive vessel barriers. Therefore, improved direct delivery methods would most likely be a better choice for these patients as they avoid significant exposure to blood components.

Despite the exciting proof of concept data generated in this rodent study, the cardiac liquid jet application requires much more detailed safety and efficacy study in large animal models. In terms of translational potential, it is conceivable that future applications could include modifying the various driving parameters with a single injector or within a multiple

injector array setup adapted to supporting instrumentation for global or regional delivery. Certainly our results are very limited to effectively targeting 1 gram of transmural myocardial mass in the rodent. In on our development course, we have identified optimized settings for a thickness level (e.g. transmural rodent cross section at 0.5cm). Our basic explanted ovine LV section application demonstrated feasibility with the same driving pressure, but at a reduced distance to achieve transmural penetration of 1.5 cm, although surface coverage was a mere 1–3mm at best per injection. Despite an optimal retention profile via adjusting to this optimal distance a much less degree of LV coverage was obtained. The problem of scale of course is evident when comparing the rodent to sheep dye results as is a problem for all delivery methods. Given that 1 g of mass was covered with 5 injections, it is very likely that >250–500 sites would be needed to achieve the same level of coverage in a human left ventricle as analogous in our sheep example. Future model studies will be needed to determine if further optimization is possible to reduce the number of sites as well as establish safety limits with a more sophisticated prototype.

A more sophisticated prototype would adjust driving pressure in real time application or with image guidance in a device configuration for an adjunctive cardiac surgery indication. For example, such a first generation liquid jet application would be suitable for AAV mediated genes encoding regeneration and or angiogenesis target locally in the peri-infarct/high risk areas. This would require a device to compute the required range of driving pressure, optimal delivery volume and be executed at a distance feasible in the surgical field. These applications would initially be limited for patients already undergoing coronary artery bypass grafts, valve replacements and ventricular assist device placements, or minimally invasive thoracic procedures. Although limited in terms of invasiveness, this patient population is significant since greater than 500,000 cardiac surgeries are performed annually, of which a large number of these patients could benefit from emerging gene therapies.

Acknowledgments

This work was supported by the National Heart Lung & Blood Institute R01 grant #2R01HL083078-05. Gracious support was received from the Gene Therapy Resource Program in providing all rAAV vectors for the animal studies. In addition we received support from the Heineman Research Foundation in Charlotte for seed funding. We also acknowledge Tracy Walling MS in the Cannon Research Center for assisting with all the histology work and Dr. Paulo Arratia at the Complex Fluids Laboratory for the device measurements.

References

1. Go AS, Mozaffarian D, Roger VL, Benjamin EJ, Berry JD, Blaha MJ, et al. Heart disease and stroke statistics--2013 update: a report from the American Heart Association. Circulation. 2014 Jan 21; 129(3):e28–e292. [PubMed: 24352519]
2. Brinks H, Koch WJ. βARKct: a therapeutic approach for improved adrenergic signaling and function in heart disease. J Cardiovasc Transl Res. 2010; 3:499–506. [PubMed: 20623214]
3. Kairouz V, Lipskaia L, Hajjar RJ, Chemaly ER. Molecular targets in heart failure gene therapy: current controversies and translational perspectives. Ann N Y Acad Sci. 2012; 1254:42–50. [PubMed: 22548568]
4. Tang T, Gao MH, Hammond HK. Prospects for gene transfer for clinical heart failure. Gene Ther. 2012; 19:606–12. [PubMed: 22534469]
5. Taimeh Z, Loughran J, Birks EJ, Bolli R. Vascular endothelial growth factor in heart failure. Nat Rev Cardiol. 2013; 10:519–30. [PubMed: 23856679]

6. Vatner SF. FGF induces hypertrophy and angiogenesis in hibernating myocardium. Circ Res. 2005; 96:705–7. [PubMed: 15831820]
7. Jaski BE, Jessup ML, Mancini DM, Cappola TP, Pauly DF, Greenberg B, Borow K, Dittrich H, Zsebo KM, Hajjar RJ. Calcium upregulation by percutaneous administration of gene therapy in cardiac disease (CUPID Trial), a first-in-human phase 1/2 clinical trial. J Card Fail. 2009; 15:171–81. [PubMed: 19327618]
8. Jessup M, Greenberg B, Mancini D, Cappola T, Pauly DF, Jaski B, et al. Calcium Upregulation by Percutaneous Administration of Gene Therapy in Cardiac Disease (CUPID): a phase 2 trial of intracoronary gene therapy of sarcoplasmic reticulum Ca2+-ATPase in patients with advanced heart failure. Circulation. 2011; 124:304–13. [PubMed: 21709064]
9. Hajjar RJ, Zsebo K, Deckelbaum L, Thompson C, Rudy J, Yaroshinsky A, et al. Design of a phase 1/2 trial of intracoronary administration of AAV1/SERCA2a in patients with heart failure. J Card Fail. 2008 Jun; 14(5):355–67. [PubMed: 18514926]
10. Greelish JP, Su LT, Lankford EB, Burkman JM, Chen H, Konig SK, et al. Stable restoration of the sarcoglycan complex in dystrophic muscle perfused with histamine and a recombinant adeno-associated viral vector. Nat Med. 1999 Apr; 5(4):439–43. [PubMed: 10202936]
11. Calcedo R, Morizono H, Wang L, McCarter R, He J, Jones D, et al. Adeno-associated virus antibody profiles in newborns, children, and adolescents. Clin Vaccine Immunol. 2011 Sep; 18(9): 1586–8. [PubMed: 21775517]
12. Boekstegers P, von Degenfeld G, Giehrl W, Kupatt C, Franz W, Steinbeck G. Myocardial gene transfer by selective pressure-regulated retroinfusion of coronary veins. Gene Ther. 2000; 7:232–240. [PubMed: 10694800]
13. Fargnoli AS, Katz MG, Yarnall C, Isidro A, Petrov M, Steuerwald N, et al. Cardiac surgical delivery of the sarcoplasmic reticulum calcium ATPase rescues myocytes in ischemic heart failure. Ann Thorac Surg. 2013 Aug; 96(2):586–95. [PubMed: 23773730]
14. Rosengart TK, Lee LY, Patel SR, Sanborn TA, Parikh M, Bergman GW, et al. Angiogenesis gene therapy: phase I assessment of direct intramyocardial administration of an adenovirus vector expressing VEGF121 cDNA to individuals with clinically significant severe coronary artery disease. Circulation. 1999 Aug 3; 100(5):468–74. [PubMed: 10430759]
15. Magovern CJ, Mack CA, Zhang J, Hahn RT, Ko W, Isom OW, et al. Direct in vivo gene transfer to canine myocardium using a replication-deficient adenovirus vector. Ann Thorac Surg. 1996 Aug; 62(2):425–33. discussion 433–4. [PubMed: 8694601]
16. Barr E, Carroll J, Kalynych AM, Tripathy SK, Kozarsky K, Wilson JM, et al. Efficient catheter-mediated gene transfer into the heart using replication-defective adenovirus. Gene Ther. 1994 Jan; 1(1):51–8. [PubMed: 7584060]
17. Matsuno Y, Iwata H, Umeda Y, Takagi H, Mori Y, Miyazaki J, et al. Nonviral gene gun mediated transfer into the beating heart. ASAIO J. 2003 Nov-Dec;49(6):641–4. [PubMed: 14655727]
18. Nishizaki K, Mazda O, Dohi Y, Kawata T, Mizuguchi K, Kitamura S, et al. In vivo gene gun-mediated transduction into rat heart with Epstein-Barr virus-based episomal vectors. Ann Thorac Surg. 2000 Oct; 70(4):1332–7. [PubMed: 11081894]
19. Le Moigne J, Mount DM, Netanyahu NS, Memarsadeghi N. A fast implementation of the ISODATA clustering algorithm. Int J Comput Geom Appl. 2007; 17:71–103.
20. Grines CL, Watkins MW, Helmer G, Penny W, Brinker J, Marmur JD, et al. Angiogenic Gene Therapy (AGENT) trial in patients with stable angina pectoris. Circulation. 2002 Mar 19; 105(11): 1291–7. [PubMed: 11901038]
21. Vale PR, Losordo DW, Milliken CE, McDonald MC, Gravelin LM, Curry CM, et al. Randomized, single-blind, placebo-controlled pilot study of catheter-based myocardial gene transfer for therapeutic angiogenesis using left ventricular electromechanical mapping in patients with chronic myocardial ischemia. Circulation. 2001 May 1; 103(17):2138–43. [PubMed: 11331253]
22. Bish LT, Sleeper MM, Brainard B, Cole S, Russell N, Withnall E, et al. Percutaneous transendocardial delivery of self-complementary adeno-associated virus 6 achieves global cardiac gene transfer in canines. Mol Ther. 2008 Dec; 16(12):1953–9. [PubMed: 18813281]

23. French BA, Mazur W, Geske RS, Bolli R. Direct in vivo gene transfer into porcine myocardium using replication-deficient adenoviral vectors. Circulation. 1994 Nov; 90(5):2414–24. [PubMed: 7525108]
24. Grossman PM, Han Z, Palasis M, Barry JJ, Lederman RJ. Incomplete retention after direct myocardial injection. Catheter Cardiovasc Interv. 2002 Mar; 55(3):392–7. [PubMed: 11870950]
25. Dixon JA, Spinale FG. Large animal models of heart failure: a critical link in the translation of basic science to clinical practice. Circ Heart Fail. 2009; 2:262–71. [PubMed: 19808348]
26. Guzman RJ, Lemarchand P, Crystal RG, Epstein SE, Finkel T. Efficient gene transfer into myocardium by direct injection of adenovirus vectors. Circ Res. 1993 Dec; 73(6):1202–7. [PubMed: 8222091]
27. von Harsdorf, Schott RJ, Shen YT, Vatner SF, Mahdavi V, Nadal-Ginard B. Gene injection into canine myocardium as a useful model for studying gene expression in the heart of large mammals. Circ Res. 1993 Mar; 72(3):688–95. [PubMed: 8431991]
28. Mays LE, Wilson JM. The complex and evolving story of T cell activation to AAV vector-encoded transgene products. Mol Ther. 2011 Jan; 19(1):16–27. [PubMed: 21119617]
29. Pfeffer MA, Braunwald E. Ventricular remodeling after myocardial infarction. Experimental observations and clinical implications. Circulation. 1990; 81:1161–1172. [PubMed: 2138525]
30. Blankinship MJ, Gregorevic P, Allen JM, Harper SQ, Harper H, Halbert CL, et al. Efficient transduction of skeletal muscle using vectors based on adeno-associated virus serotype 6. Mol Ther. 2004 Oct; 10(4):671–8. [PubMed: 15451451]
31. Wang Z, Zhu T, Qiao C, Zhou L, Wang B, Zhang J, et al. Adeno-associated virus serotype 8 efficiently delivers genes to muscle and heart. Nat Biotechnol. 2005 Mar; 23(3):321–8. [PubMed: 15735640]
32. Boekstegers P, Kupatt C. Current concepts and applications of coronary venous retroinfusions. Bas Res Card. 2004; 99:373–381.
33. Byrne MJ, Power JM, Preovolos A, Mariani JA, Hajjar RJ, Kaye DM. Recirculating cardiac delivery of AAV2/1SERCA2a improves myocardial function in an experimental model of heart failure in large animals. Gene Ther. 2008 Dec; 15(23):1550–7. [PubMed: 18650850]
34. Liu Q, Huang W, Zhang H, Wang Y, Zhao J, Song A, et al. Neutralizing antibodies against AAV2, AAV5 and AAV8 in healthy and HIV-1-infected subjects in China: implications for gene therapy using AAV vectors. Gene Ther. 2014 May 22.

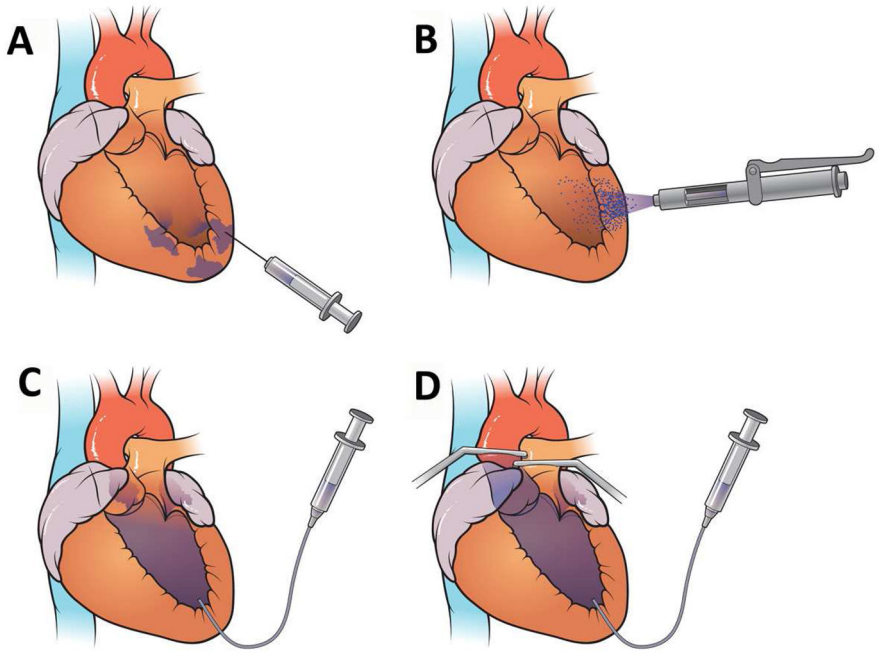

Figure 1.

Cardiac Gene Delivery Methods (A) IM Injection (B) Liquid Jet Injection Delivery (C) Intra left ventricular cavitary Infusion LVIC (D) Infusion featuring dual occlusion of aortic and pulmonary vessels LVIC-OCCL

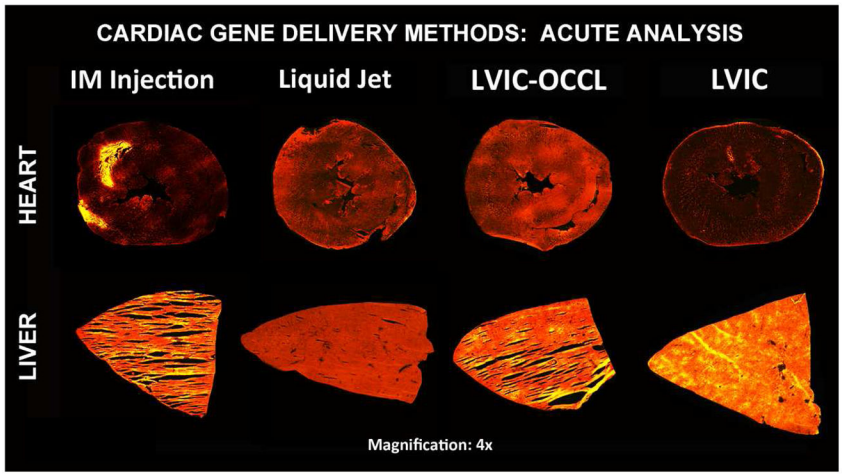

Figure 2.

Myocardial and Liver Cross Section Acute Study Results [4x magnification] By Group IM Injection, Liquid Jet Delivery, LVIC-OCCL and LVIC Infusion. Rhodamin B dye fluorescence (red-yellow intensity) demonstrated in myocardial cross sections (top) and systemic exposure in the liver sections (bottom). The delivery route had a significant impact on retention and the resultant intensity distribution profile immediately after 10 minutes.

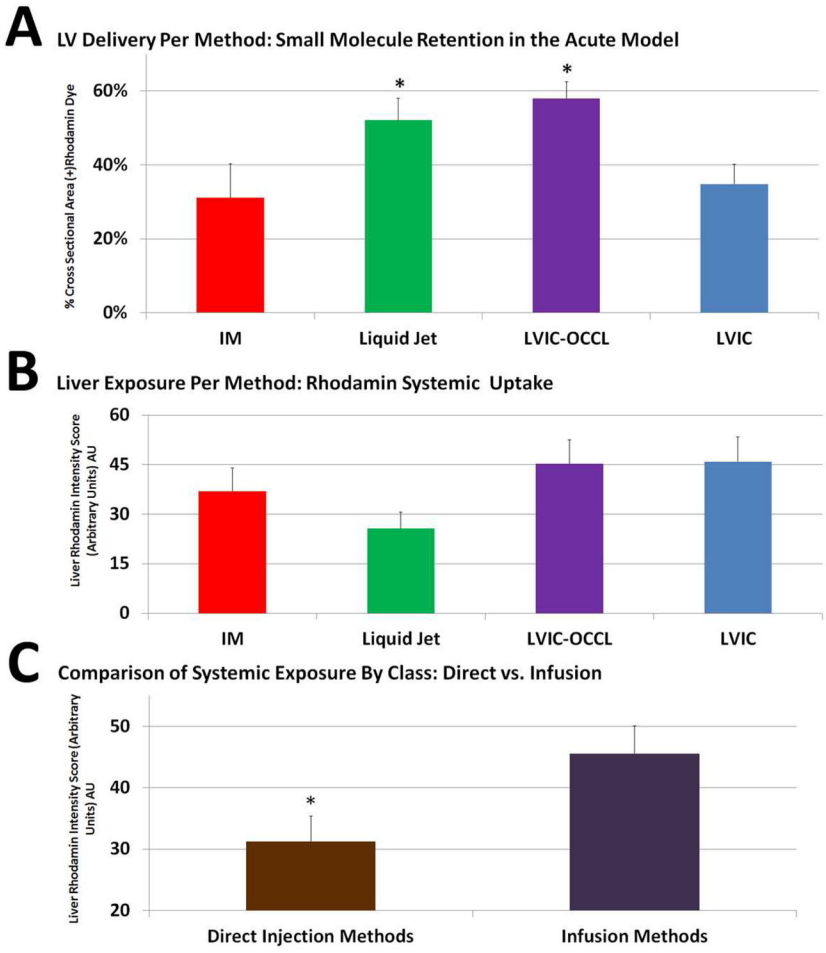

Figure 3.

Acute Model Results: (A) Liquid Jet and LVIC-OCCL demonstrate significantly greater retention versus both IM and LVIC groups * $p<0.05$ confidence level via Tukey's test. (B) All groups resulted in systemic exposure (C) Direct methods, IM and Liquid Jet combined demonstrate lower overall exposure versus Infusion methods or LVIC-OCCL and LVIC combined, * $p<0.05$.

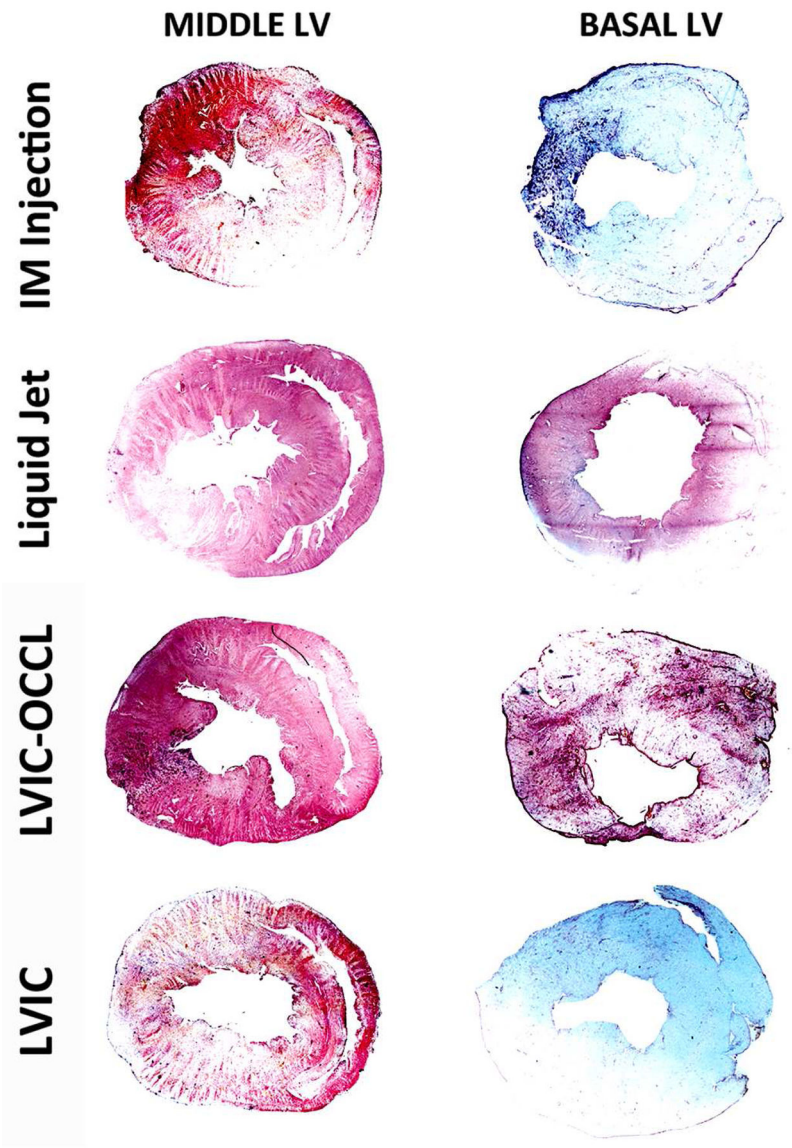

Figure 4.

Left Ventricular Cross Section GFP Expression Distribution Per Delivery Method [4x magnification]. Top to Bottom, IM Injection, Liquid Jet, LVIC-OCCL and LVIC AAV groups. Immunohistochemistry revels EGFP (purple-brown) detection while (white-blue) regions are void. EGFP Expression profiles presented in the Middle and Basal LV sections (left to right) per group with 2D myocardial area coverage expressed as a %.

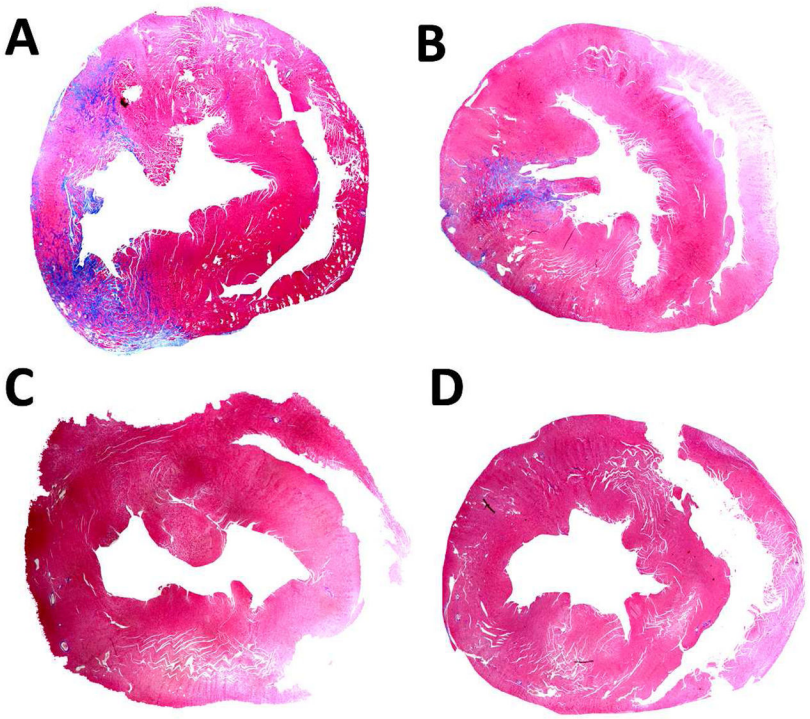

Figure 5.

Masson's Trichrome staining results indicating myocardial damage per delivery method, blue area indicates (+) LV fibrosis regions. The IM injection (A) and LVIC-OCCL (B) groups impose moderate left ventricular damage following delivery while the Liquid Jet (C) and LVIC (D) groups did not present with any indication of fibrosis.

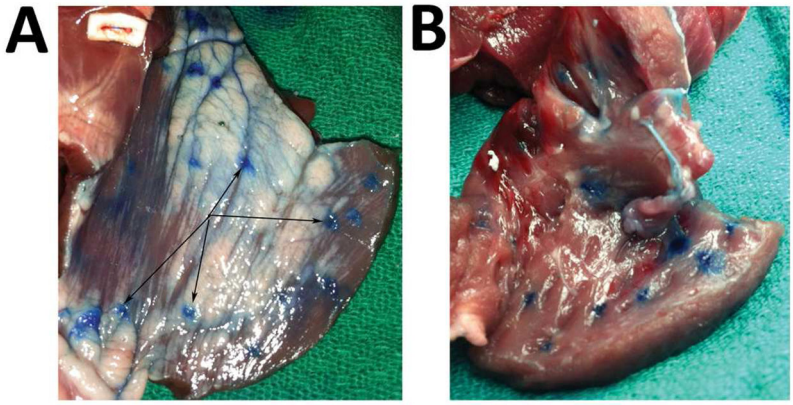

Figure 6.

Ex Vivo Ovine Methylene Blue Results for translational potential of needleless liquid jet injection (A) Liquid Jet entry points located on the epicardial surface demonstrate the jet's local, yet dispersive profile along the adjacent surface contours and (B) robust transmural delivery retained per injection site within the endocardial surface.